

# Synthesis and photoluminescence properties of Eu<sup>3+</sup>-activated SrZnO<sub>2</sub>

P. J. Purohit · M. Mohapatra · V. Natarajan · S. V. Godbole

Received: 25 August 2010/Accepted: 25 October 2010/Published online: 6 November 2010  
© Springer Science+Business Media, LLC 2010

**Abstract** Synthesis, X-ray diffraction, and photoluminescence (PL) investigations of SrZnO<sub>2</sub> doped with Eu<sup>3+</sup> were carried out in order to characterize the material. The emission spectra showed a broad band emission at 525 nm attributed to oxygen defect centers in the host matrix, along with peaks corresponding to the  $^5D_0 \rightarrow ^7F_j$  ( $j = 1, 2$ ) transitions of Eu ion under 250 nm excitation. PL decay time studies were done to confirm these investigations. Time-resolved emission spectrometric (TRES) study was carried out to extract the emission spectra of the Eu ion which was buried under the broad band emission. After giving suitable delay times and by choosing a proper time gate, transitions due to  $^5D_0 \rightarrow ^7F_j$  ( $j = 0, 1, 2, 3$ , and 4) could be observed. Judd–Ofelt intensity parameters and other radiative properties for the system were evaluated from this emission spectrum and decay time data by adopting standard procedure. The color coordinates of the system were also evaluated and plotted on a standard CIE index diagram. The observations showed that the SrZnO<sub>2</sub>:Eu<sup>3+</sup> material has near white light emission (also considering the emission from host) whereas, the extracted emission spectrum due to only Eu ions has a near red emission.

## Introduction

During the last few decades, rare-earth-activated oxide based phosphors have led to a revolution in lighting

industry [1]. In particular, the remarkable narrow-band emission properties of trivalent rare-earth (RE) ions such as Eu<sup>2+</sup>/Eu<sup>3+</sup>, Tb<sup>3+</sup>, Dy<sup>3+</sup>, Ce<sup>3+</sup> ions, etc. have been utilized to the maximum extent in the development of efficient phosphors for lamps, plasma display panels, and also for light-emitting diodes(LEDs) [2–4]. Recently, several reports have appeared in literature regarding the novel compound SrZnO<sub>2</sub> and its utility as an oxide-based host for phosphor material [5–13]. But the first report on use of this host for luminescent applications can be attributed to Kubota et al. [6], where they had investigated on the application of Ba<sup>2+</sup> and Mn<sup>2+</sup>-doped SrZnO<sub>2</sub> system as a luminescent material. Later, He et al. reported the luminescence performance of the host as a red and blue-green emitting phosphor, when doped with Eu<sup>3+</sup> and Pr<sup>3+</sup> ions, respectively [7, 8]. Khatkar et al. and Yu et al. have reported the utility of the host material as a blue-green phosphor by doping with Tb<sup>3+</sup> [9, 10]. Yang et al. [11] have reported the photoluminescence (PL) investigation of the Sm-doped strontium zinc oxide system. Eu<sup>3+</sup> doped in this host was shown to be a potential red emitting phosphor by Wang and Gao [12]. Also, Yu et al. have reported the PL properties of Eu<sup>3+</sup> ion codoped with several alkali metals in this phosphor host [13]. These reports proved the utility of SrZnO<sub>2</sub> as a potential host material for phosphors. However, all these reports did not throw any light on the symmetry of the metal ions in this matrix and the various emission properties associated with it. The present study was initiated to investigate the emission spectra of the Eu metal ion in the oxide host and comment on its symmetry by adopting standard Judd–Ofelt (J–O) analysis. We observed white light emission from the Eu-doped sample, which is unusual for this host. A detailed investigation in this regard is presented in this paper. Along with these studies, various radiative properties such as the J–O

P. J. Purohit · M. Mohapatra · V. Natarajan (✉) · S. V. Godbole  
Radiochemistry Division, Bhabha Atomic Research Centre,  
Trombay, Mumbai 400085, India  
e-mail: vnatra@yahoo.co.in

intensity parameters, luminescence branching ratios, radiative probabilities and lifetimes, quantum efficiency, etc. were also determined from the emission and lifetime data that are presented here. These parameters reflect the local structure around the metal ion and provide information regarding nature of the metal–ligand bonding in the matrix. Apart from this, the color coordinates for the system were also calculated adopting standard procedure and plotted on the standard CIE index diagram.

## Experimental

All the chemicals used were of AR grade. The undoped SrZnO<sub>2</sub> samples were prepared via high temperature solid-state reaction route as discussed below. Stoichiometric quantities of SrCO<sub>3</sub> and Zn(CH<sub>3</sub>COO)<sub>2</sub> were mixed thoroughly and ground in an agate mortar. The mixture was heated first at 500 °C for 4 h so as to obtain a gray colored product. Later this sample was heated at 900 and 1,000 °C for 3 h. This was cooled to room temperature and further ground to obtain a white powder. This powder was heated at 1,300 °C for 2 h. The product thus obtained was used for further investigations. Eu-doped sample was prepared by mixing appropriate quantities of 99.99% pure Eu<sub>2</sub>O<sub>3</sub> at the starting point following similar steps so that the metal ion concentration was 1 mol%. Phase purity of the samples was examined by X-ray diffraction (XRD) measurements carried out on a STOE X-ray diffractometer using a Ni filter and graphite monochromator. The diffraction patterns were obtained using monochromatic Cu-K<sub>α1</sub> radiation ( $\lambda = 1.5406 \text{ \AA}$ ), keeping the scan rate at 0.05°/s in the scattering angle range ( $2\theta$ ) of 20° to 60°. The XRD patterns obtained were then compared with the standard ICDD files. The PL emission and lifetime (decay time) data were recorded on an Edinburgh CD-920 unit equipped with Xe flash lamp as the excitation source. The acquisition and analysis of the data were done by F-900 software provided by Edinburgh Analytical Instruments, UK.

## Results and discussion

### XRD data

Figure 1 shows the XRD patterns of the SrZnO<sub>2</sub> samples after annealing the samples at 900 °C (a) and 1,300 °C (b). In the sample heated at 900 °C, peaks corresponding to unreacted ZnO ( $2\theta = 31.75^\circ, 36.25^\circ, 34.35^\circ, 47.50^\circ$ , and  $56.55^\circ$ ) and SrCO<sub>3</sub> ( $2\theta = 27.55^\circ$ ) were also observed along with the peaks due to SrZnO<sub>2</sub>. However, in the sample heated at 1,300 °C, no impurity phase was observed. The observed patterns were matched with that of

SrZnO<sub>2</sub> crystallized in an orthorhombic geometry with space group *Pnma* (ICDD file no-41-0551, shown in Fig. 1c). The XRD data was indexed on an orthorhombic system with cell parameters  $a = 0.5850$ ,  $b = 0.3310$ , and  $c = 1.1338 \text{ nm}$  which are shown in Table 1.

The crystal structure of SrZnO<sub>2</sub> has been reported by Schnerring and Hoppe [14, 15].

SrZnO<sub>2</sub> structure is a layered one consisting of ZnO<sub>4</sub> tetrahedra sharing its edges with one another. The Sr atoms are located in between these layered layers. There is one site for the Sr atom where it is surrounded by seven oxygen atoms. Also there is one site for the Zn atom but two sites for the oxygen atoms.

The ionic radii of Zn<sup>2+</sup>, Sr<sup>2+</sup>, and Eu<sup>3+</sup> are 74, 121, and 95 pm, respectively. On doping the oxide system with the Eu<sup>3+</sup> ion, it could replace the Sr<sup>2+</sup> or Zn<sup>2+</sup> ion, though the former is more favored. In order to keep the charge balance, two Eu<sup>3+</sup> ions will be needed to substitute for three

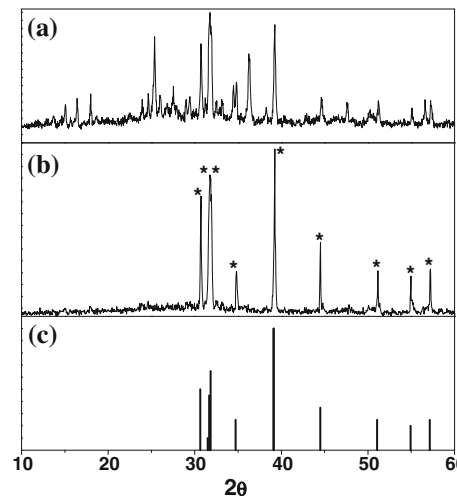


**Fig. 1** XRD patterns of the undoped SrZnO<sub>2</sub> samples; **a** after 900 °C heat treatment and **b** after 1,300 °C heat treatment. The standard ICDD stick patterns that matched with the experimental patterns is shown in **c**. The peaks with asterisk mark are due to pure SrZnO<sub>2</sub>

**Table 1** XRD data of SrZnO<sub>2</sub> ( $\lambda = 0.15406 \text{ nm}$ )

$2\theta$ values	$d$ value (Å)	$I/I_0$	$h\ k\ l$
30.65	2.91	50	2 0 0
31.65	2.82	45	2 0 1
31.80	2.80	65	1 1 1
34.70	2.58	25	1 1 2
39.10	2.30	100	1 1 3
44.50	2.03	35	2 0 4
51.05	1.78	25	1 1 5
54.90	1.67	20	0 2 0
57.15	1.61	25	3 1 2

divalent ions. Hence, one vacancy (defect centre) with two negative charges and two positive defects would be created.

#### PL emission data

Figure 2(b) shows the emission spectrum of the Eu incorporated  $\text{SrZnO}_2$  with 250 nm excitation. The spectrum shows a very broad peak ranging from 450 to 650 nm with maximum at 525 nm. Over this broad band, few sharp transitions were observed at 590 and 614 nm. The peaks at 592 and 612 nm are the well known  $\text{Eu}^{3+}$  emissions in the orange and red regions, respectively. The host  $\text{SrZnO}_2$  heated at 1,300 °C also showed this broad emission peaking at 525 nm (Fig. 2(a)).

The excitation spectrum corresponding to the 592 nm emission of the undoped and Eu-doped sample is shown in Fig. 3. The intense peak observed in both the samples at ~230 nm was assigned to the host absorption. The broad band observed in the Eu-doped sample at 250 nm was attributed to  $\text{Eu}^{3+}$  charge transfer (CT) transition [12, 16]. And the peaks seen at 320, 365, 380, and 395 nm were assigned to the f-f transitions from the  $^7\text{F}_0$  ground state to  $^5\text{H}_3$ ,  $^5\text{L}_9$ ,  $^5\text{G}_3$ , and  $^5\text{L}_6$  levels, respectively.

The broad emission peak observed in our samples has not been reported in earlier reports of  $\text{SrZnO}_2:\text{Eu}^{3+}$ . Though similar broad emission around 530 nm has been reported by Zhang et al. in ZnO nano-powders [17], the corresponding excitation peak was observed at 385 nm. In the present study, the excitation peak of the undoped sample corresponds to 230 nm. Therefore, we strongly believe that the broad emission at 525 nm observed in our samples arises only due to electron transitions mediated by defect levels (e.g., oxygen vacancies) in band gap of  $\text{SrZnO}_2$  lattice.

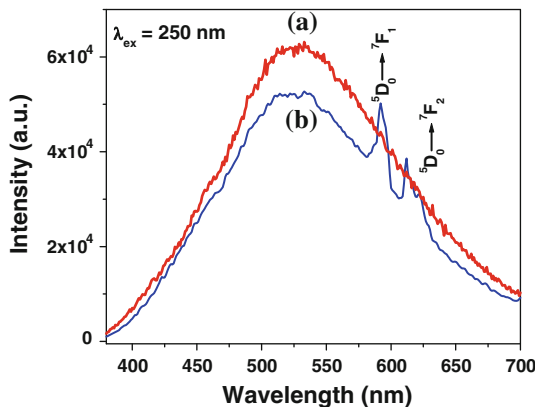


**Fig. 2** *a* emission from the host and *b* emission spectrum of the  $\text{SrZnO}_2:\text{Eu}$  with  $\lambda_{\text{ex}} = 250$  nm

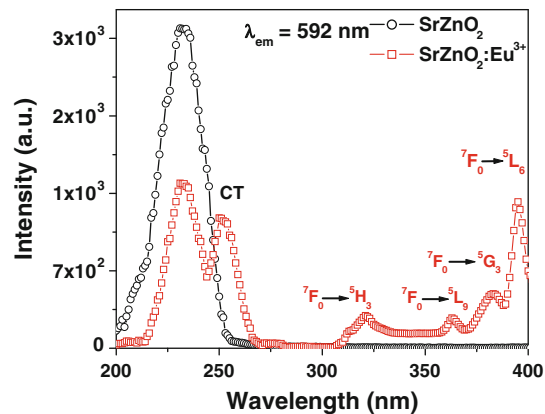


**Fig. 3** Excitation spectrum of the host with  $\lambda_{\text{em}} = 525$  nm and  $\text{SrZnO}_2:\text{Eu}$  with  $\lambda_{\text{em}} = 592$  nm

#### PL decay time data

To probe further into the luminescence properties of the dopant ion, fluorescence decay time studies were carried out on the sample. The luminescence decay time curve for the  $\text{Eu}^{3+}$ -doped sample recorded with  $\lambda_{\text{ex}} = 250$  nm and  $\lambda_{\text{em}} = 612$  nm is shown in Fig. 4. The luminescence decay curve was recorded on 20 ms scale and fitted using the following exponential decay equation.

$$I(t) = A_i + \sum_{i=1}^n e^{\frac{t}{\tau_i}} \quad (1)$$

Here  $A_i$  are scalar quantities,  $t_i$  are the times of measurement, and  $\tau_i$  are the decay time values (i.e., the time taken for the excited state population to become  $1/e$  of the original value). The decay curve could be fitted into a bi-exponential decay whose major component (>95%) was 1.8 ms and minor component was 0.158 ms with the parameter of fitting  $\chi^2 = 1.514$ . The life time of the broad

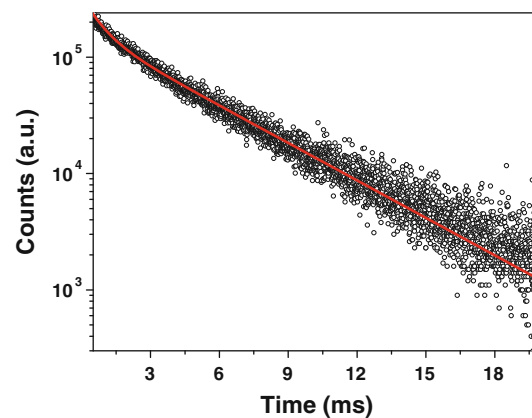


**Fig. 4** PL decay time profile of the Eu-doped sample with  $\lambda_{\text{ex}} = 250$  nm and  $\lambda_{\text{em}} = 612$  nm. The dots represent the observed points and the solid line gives its exponential fitting

band emission at 525 nm emission was also observed to be 0.16 ms. This confirms the fact that, the initial short lived component observed in the 1–3 ms range in Fig. 4 is due to the tail portion of the broad band host emission.

In order to extract the spectra due to  $\text{Eu}^{3+}$  only, a time-resolved emission spectrometry (TRES) method was adopted, where in a set of emission scans were obtained by giving suitable delay times and choosing a proper time gate. Figure 5 represents the TRES spectra of the strontium zinc oxide samples doped with Eu obtained at various delay times and with  $\lambda_{\text{ex}} = 250 \text{ nm}$ .

It is clear from the spectra that after giving a delay time of 300  $\mu\text{s}$ , the intensity of the broad peak at 525 nm (attributed to oxygen related defect centres) is drastically reduced and a clear spectrum for the  $\text{Eu}^{3+}$  could be seen. The spectrum obtained after a time delay of 700  $\mu\text{s}$  was further used for the emission data analysis and calculation of J–O parameters (shown in Fig. 6). This spectrum consists of a number of sharp lines at 580, 592, 611, 651, and 692–711 nm, which are associated with the transitions from the excited  $^5\text{D}_0$  to  $^7\text{F}_J$  levels of  $\text{Eu}^{3+}$  where  $J = 0, 1, 2, 3$ , and 4, respectively.

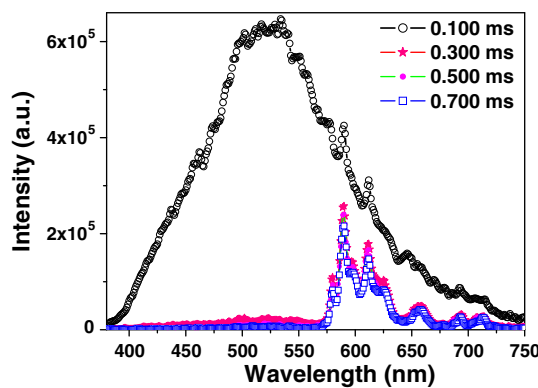


**Fig. 5** TRES spectra of the  $\text{Eu}^{3+}$ -doped  $\text{SrZnO}_2$  samples after suitable delay times with  $\lambda_{\text{ex}} = 250 \text{ nm}$

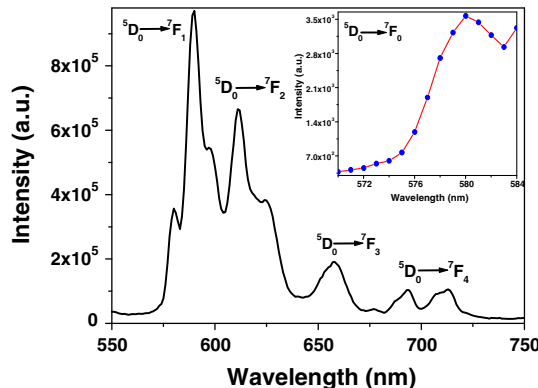


**Fig. 6** Emission spectrum of  $\text{SrZnO}_2:\text{Eu}^{3+}$  with  $\lambda_{\text{ex}} = 250 \text{ nm}$  obtained after a delay of 700  $\mu\text{s}$ . The inset figure shows the  $^5\text{D}_0$  to  $^7\text{F}_0$  transition at 580 nm

Here, the red emission at 611 nm involving  $\Delta J = \pm 2$  transition is an electric-dipole transition, while the orange emission at 590 nm is a typical magnetic dipole allowed transition ( $\Delta J = \pm 1$ ).

#### Evaluation of J–O parameters of the $\text{Eu}^{3+}$ sample

The Judd–Ofelt analysis of the emission spectrum is a powerful tool for calculating the parity-forbidden electric-dipole radiative transition rates between the various levels of a rare-earth ion such as  $\text{Eu}^{3+}$  [18, 19]. Through these analyses, the local environment around the metal ion and the bond covalency of M–L bonds can be interpreted. Apart from this, the radiative transition rate ( $A_R$ ), radiative lifetimes ( $\tau_R$ ), and luminescence branching ratios ( $\beta_R$ ) can also be computed. It is possible to determine the J–O intensity parameters  $\Omega_J$  (where  $J = 2, 4, 6$ , etc.) based on the emission spectral data as shown by various authors [20–23].

For a particular transition, the emission intensity ( $I$ ) can be considered as proportional to the area under the emission curve for that transition. Also, the intensity will be proportional to the radiative decay rate of the transition ( $A_R$ ).

$$I = hc\nu A_R N \alpha (\text{Area under the curve}) \quad (2)$$

Here  $hc\nu$  is the energy separation in the initial and final levels and  $N$  is the population of the  $^5\text{D}_0$  level (in case of  $\text{Eu}^{3+}$ ). The  $^5\text{D}_0 \rightarrow ^7\text{F}_{2, 4, 6}$  transitions are electric dipole allowed whose radiative decay rates can be represented by the following equations as shown by Malta et al. [24, 25].

$$A_{R(\text{ed})} = \left\{ \left( \frac{64\pi^4 e^2 v^3}{3h(2J+1)} \right) \frac{n(n^2+2)^2}{9} \right\} \sum_J \Omega_J \langle \|U^{(J)}\| \rangle^2 \quad (3)$$

Here the factor  $\frac{n(n^2+2)^2}{9}$  is the Lorentz local field correction that converts the external electromagnetic field into an effective field at the location of the active center in the dielectric medium and  $n$  is the refractive index of the medium.  $\|U^{(J)}\|$  are the doubly reduced matrix elements corresponding to the  $^5\text{D}_0 \rightarrow ^7\text{F}_J$  transitions of the metal ion;  $e$  is the electron charge and  $v$  is the transition energy in  $\text{cm}^{-1}$ . Neglecting the J–J mixing, it is found that, the intensities of the transitions solely depend on the respective matrix elements.

For the present strontium zincate system, the index of refraction was calculated by standard Gladstone and Dale formula as suggested by Larsen and Burman [26] and illustrated in Lange's Hand book of Chemistry [27].

For the calculations of  $\Omega_J$  values in Eu-doped  $\text{SrZnO}_2$  system, the intensity of  $^5\text{D}_0 \rightarrow ^7\text{F}_1$  transition, which is a magnetic dipole allowed transition, was taken as the

reference. The transition rate ( $A_{R(\text{md})}$ ) of this magnetic dipole allowed transition is represented by the following equation [28].

$$(A_{R(\text{md})}) = \left\{ \left( \frac{64\pi^4 v^3}{3h(2J+2)} \right) \right\} n^3 S_{\text{md}} \quad (4)$$

Here  $S_{\text{md}}$  is the magnetic-dipolar transition line strength and is independent of host matrix. For the present system, its value was taken as  $9.6 \times 10^{-42}$  esu<sup>2</sup> cm<sup>2</sup> as reported by Werts et al. and Weber et al. [22, 29].

The total radiative decay rate ( $A_R$ ) value was calculated from the ratio of the sum of the areas under the  ${}^5D_0 \rightarrow {}^7F_J$  transitions ( $\sum \int I_J dv$ ), to area under the curve of the  ${}^5D_0 \rightarrow {}^7F_1$  transition ( $\int I_1 dv$ ).

$$\frac{\left( \sum \int I_J dv \right)}{\left( \int I_1 dv \right)} = \frac{A_R}{A_{R\text{md}}} \quad (5)$$

The J–O intensity parameters,  $\Omega_J$  were calculated from the respective  $A_{\text{Red}}$  values as per Eq. 3. The values for the reduced square matrix elements ( $\|U^{(J)}\|$ ) for the  ${}^7F_2$  and  ${}^7F_4$  transitions were taken as 0.0032 and 0.0023, respectively [22, 30–32].

Since, the  ${}^5D_0 \rightarrow {}^7F_6$  transition was not observed in the present case, its J–O parameters could not be evaluated.

The total radiative lifetime can be represented as the reciprocal of the total radiative decay rate, i.e.,  $\tau_R = \frac{1}{A_R}$ . From the experimental decay time ( $\tau_f$ ) and  $\tau_R$  values, the  $\tau_{\text{NR}}$ , i.e., the non radiative life time was calculated by the following formula.

$$\frac{1}{\tau_f} = \frac{1}{\tau_R} + \frac{1}{\tau_{\text{NR}}} \quad (6)$$

Similarly, the branching ratios ( $\beta_J = \frac{A_J}{\sum A_J}$ ) for the different excited states and the overall quantum efficiency ( $\eta = \frac{\tau_R}{\tau_f}$ ) were calculated by standard procedures. All these parameters for the Eu<sup>3+</sup> ion in the zincate host are listed in Table 2.

$\Omega_2$  exhibits dependence on the covalence between rare-earth ions and ligands and gives information about the asymmetry of the local environment of Eu<sup>3+</sup> site. The trend

**Table 3** Comparison of the J–O intensity parameters of Eu<sup>3+</sup>-doped SrZnO<sub>2</sub> with that of other hosts

Host	$\Omega_2$ (10 <sup>-20</sup> cm <sup>2</sup> )	$\Omega_4$ (10 <sup>-20</sup> cm <sup>2</sup> )	References
Strontium zincate	3.60	1.35	Present study
Strontium meta phosphate	5.9	1.4	[35]
Strontium barium niobate	2.1	3.8	[36]
Zinc phosphate	5.8	2.3	[37]

observed in the J–O parameters here ( $\Omega_2 > \Omega_4$ ) confirms the covalency existing between the rare-earth ion (Eu<sup>3+</sup>) and ligands as well as the asymmetry around the metal ion site. The  ${}^5D_0 \rightarrow {}^7F_3$  transition cannot be accounted for by either the magnetic or electric-dipole mechanisms. Its presence is considered to be a small deviation from theory at the level used in this study. However, some workers say that these transitions “borrow” intensity from the  ${}^5D_0 \rightarrow {}^7F_2$  transitions through higher order perturbations by the crystal field and show bands in the emission spectrum [21]. A comparison of the J–O intensity parameters of the strontium zincate system with that of other hosts is presented in Table 3.

#### Evaluation of color coordinates

In order to evaluate the material performance on color luminescent emission, CIE chromaticity coordinates were evaluated adopting standard procedures [33, 34]. The values of  $x$  and  $y$  coordinates of the system were calculated to be 0.324 and 0.421, respectively. This is represented as the point “b” in the CIE diagram. For an ideal white light phosphor system, the values are 0.33 and 0.33, respectively (represented as the “achromatic point”, “a” in the CIE index diagram, Fig. 7). It is clear from the values that, the SrZnO<sub>2</sub>:Eu<sup>3+</sup> system, gives a near white light emission when excited at 250 nm. On the other hand, when the emission spectrum obtained after giving 700 μs is taken into consideration, the CIE coordinates are calculated to be 0.571 and 0.386, respectively (point “c”) suggesting a near “RED” emission.

**Table 2** J–O intensity parameters and radiative properties of the Eu<sup>3+</sup>-doped SrZnO<sub>2</sub>

Transition	$A_{\text{Red}}$ (s <sup>-1</sup> )	$A_{R\text{md}}$ (s <sup>-1</sup> )	$\Omega_J$ (10 <sup>-20</sup> cm <sup>2</sup> )	$\beta_J$ (%)	$\eta$ (%)	$A_{\text{total}}$ (s <sup>-1</sup> )	$\tau_R$ (μs)
${}^5D_0 \rightarrow {}^7F_1$	0	72.1	–	25.0	52	290	350
${}^5D_0 \rightarrow {}^7F_2$	135	0	3.60	47.5			
${}^5D_0 \rightarrow {}^7F_4$	34.5	0	1.35	27.5			

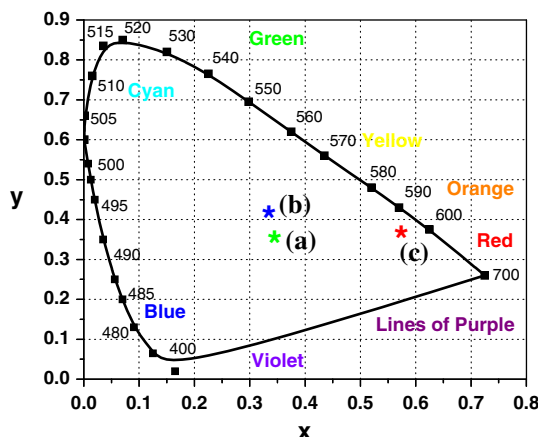


**Fig. 7** CIE chromaticity diagram for  $\text{Eu}^{3+}$ -doped  $\text{SrZnO}_2$  system. Point a: corresponds to an ideal white light phosphor system. Point b: shows the values for the  $\text{Eu}^{3+}$ -doped  $\text{SrZnO}_2$ . Point c: corresponds to the emission obtained after  $700 \mu\text{s}$

## Conclusion

$\text{SrZnO}_2$  samples doped with Eu ions were prepared via solid state reaction route. XRD studies confirmed the formation of a single phase compound after heat treatment at  $1,300^\circ\text{C}$ . The emission spectra of the sample showed a broad band at  $525 \text{ nm}$  attributed to oxygen defect centers in the host matrix, along with peaks corresponding to the  $^5\text{D}_0 \rightarrow ^7\text{F}_J$  ( $J = 1, 2$ ) transitions of Eu ion under  $250 \text{ nm}$  excitation. The PL decay time studies were done to confirm these investigations. A TRES study was carried out to extract the emission spectra of the Eu ion which was buried under the broad band emission. After giving suitable delay times and by choosing a proper time gate, transitions due to  $^5\text{D}_0 \rightarrow ^7\text{F}_J$  ( $J = 0, 1, 2, 3$ , and  $4$ ) could be observed. Various emissive properties such as J-O intensity parameters, radiative transition rates and life times, luminescence branching ratios, and quantum efficiency for the system were calculated adopting standard procedure. The color coordinates of the system were also evaluated and plotted on a standard CIE index diagram. The observations showed that the  $\text{SrZnO}_2:\text{Eu}^{3+}$  material has near white light emission (also considering the emission from host) whereas, the extracted emission spectrum due to only Eu ions has a near red emission.

## References

1. Blasse G (1989) Chem Mater 1:294
2. He X-H, Lian N, Sun J-H, Guan M-Y (2009) J Mater Sci 44:4763. doi:[10.1007/s10853-009-3668-4](https://doi.org/10.1007/s10853-009-3668-4)
3. Wang H, Yu J, Li J, Cheng X, Huang Z (2010) J Mater Sci 45:1237. doi:[10.1007/s10853-009-4072-9](https://doi.org/10.1007/s10853-009-4072-9)
4. Shan Z, Chen D, Yu Y, Huang P, Lin H, Wang Y (2010) J Mater Sci 45:2775. doi:[10.1007/s10853-010-4266-1](https://doi.org/10.1007/s10853-010-4266-1)
5. Taikar DR, Joshi CP, Moharil SV, Muthal PL, Dhopte SM (2010) J Lumin 130:1690
6. Kubota S, Oyama T, Yamane H, Shimada M (2003) Chem Mater 15:3403
7. He XH, Zhou J, Li WH, Zhou QF (2006) Chin J Inorg Chem 22:1706
8. He XH, Zhou J, Bi CL, Li WH (2007) J Synth Cryst 36:1408
9. Khatkar SP, Taxak VB, Kumar D, Han SD, Han CH, Sharma G (2006) J Korean Phys Soc 48:1355
10. Yu X, Xu X, Zhou P, Peng X, Yang S (2005) Mater Lett 59:1178
11. Yang L, Yu X, Yang S, Zhou C, Zhou P, Gao W, Ye P (2008) Mater Lett 62:907
12. Wang Y, Gao H (2006) J Solid State Chem 179:1870
13. Yu X, Xu X, Zhou C, Tang J, Peng X, Yang S (2006) Mater Res Bull 41:1578
14. von Schnering HG, Hoppe R (1960) Naturwissenschaften 47:467
15. von Schnering HG, Hoppe R (1961) Z Anorg Allg Chem 312:87
16. Chen XY, Liu GK (2005) J Solid State Chem 178:419
17. Zhang LL, Guo CX, Zhao JJ, Hu JT (2005) Chin Phys Lett 22:1225
18. Judd BR (1962) Phys Rev 127:750
19. Ofelt GS (1962) J Chem Phys 37:511
20. Sarakha L, Forano C, Boutinaud P (2009) Opt Mater 31:562
21. Liu L, Chen X (2007) Nanotechnol 18:255704
22. Werts MHV, Jukes RTF, Verhoeven JW (2002) Phys Chem Chem Phys 4:1542
23. Shipeng W, Xiaoping Z, Shui H, Liqun Z, Li L (2008) J Rare Earths 26:787
24. Malta OL, Brito HF, Menezes JFS, Goncalves e silva FR, Alves S Jr, Farias FS Jr, De Andrade AVM Jr (1997) J Lumin 75:255
25. Malta OL, Couto dos Santos MA, Thompson LC, Ito NK (1996) J Lumin 69:77
26. Larsen ES, Berman H (1934) The microscopic determination of the non-opaque minerals, 2nd edn. U.S. Geological Survey Bulletin, Washington, DC, p 848
27. Dean JA (ed) (1973) LANGE's handbook of chemistry, 11th edn, 10.258. McGraw-Hill Book Company, New York
28. Heidepriem HE, Ehrt D (1996) J Non-Cryst Solids 208:205
29. Weber MJ, Varitimos TE, Matsinger BH (1973) Phys Rev B 8:47
30. Carnall WT, Fields PR, Rajnak K (1968) J Chem Phys 49:4450
31. Kuboniwa S, Hoshina T (1972) J Phys Soc Jpn 32:1059
32. Carnall WT, Fields PR, Wybourne BG (1965) J Chem Phys 42:3797
33. Publication CIE No. 7.4 (1987) International Lighting Vocabulary. Central Bureau of the Commission Internationale de L'Éclairage, Vienna, Austria
34. Publication CIE No. 15.2 (1986) Colorimetry, 2nd edn. Central Bureau of the Commission Internationale de L'Éclairage, Vienna, Austria
35. Zaccaria S, Casarin M, Speghini A, Ajo D, Bettinelli M (1999) Spectrochim Acta A 55:171
36. Andresen Å, Bahar AN, Conradi D, Oprea II, Pankrath R, Voelker U, Betzler K, Wöhlecke M, Caldiño U, Martín E, Jaque D, Solé JG (2008) Phys Rev B 77:214102
37. Capobianco JA, Proulx PP, Bettinelli M, Negrisolo F (1990) Phys Rev B 42:5936